PMMW IMAGE SUPER RESOLUTION FROM COMPRESSED SENSING OBSERVATIONS

Wael Saafin[1], Salvador Villena[2], Miguel Vega[2], Rafael Molina[1], and Aggelos K. Katsaggelos[3]

[1] Dept. of Computer Science and Artificial Intellegence, University of Granada, Granada, Spain.
[2] Dept. of Languages and Information Systems, University of Granada, Granada, Spain.
[3] Dept. of Electrical Engineering and Computer Science, Northwestern University, Evanston, USA
waelsaafin@correo.ugr.es, {svillena,mvega}@ugr.es, rms@decsai.ugr.es, aggk@eecs.northwestern.edu

ABSTRACT

In this paper we propose a novel optimization framework to obtain High Resolution (HR) Passive Millimeter Wave (PMMW) images from multiple Low Resolution (LR) observations captured using a simulated Compressed Sensing (CS) imaging system. The proposed CS Super Resolution (CSSR) approach combines existing CS reconstruction algorithms with the use of Super Gaussian (SG) regularization terms on the image to be reconstructed, smoothness constraints on the registration parameters to be estimated and the use of the Alternate Direction Methods of Multipliers (ADMM) to link the CS and SR problems. The image estimation subproblem is solved using *Majorization-Minimization* (MM), registration is tackled minimizing a quadratic function and CS reconstruction is approached as an l_1-minimization problem subject to a quadratic constraint. The performed experiments, on simulated and real PMMW observations, validate the used approach.

Index Terms— Passive millimeter-wave, compressive sensing, super resolution, image restoration

1. INTRODUCTION

Due to their characteristics, MMW images are used in applications like weather operations, low visibility navigation, and the imaging of people for concealed object and threat detection [1, 2, 3], just to name a few.

Based on their interest, image processing techniques have recently started to be applied to these images. For instance, Passive Millimeter Wave (PMMW) image enhancement has been addressed in [4]. In [5] the high frequency components of those images were restored using a MAP estimator, and they were then added to the input image to produce a HR image. Registration and fusion of visible and MM images as well as segmentation of MMW images have been addressed in [2, 6, 7].

This paper has been supported by The European Union, Erasmus Mundus program, the Spanish Ministry of Economy and Competitiveness under project TIN2013-43880-R, the European Regional Development Fund (FEDER), the CEI BioTic at the Universidad de Granada, and the Department of Energy (DE-NA0002520).

Unfortunately PMMW systems have two serious shortcomings: the long acquisition time needed to produce a PMMW image and the poor resolution of captured images. CS systems, with its reduced image acquisition time, have been applied to PMMW imaging, see[8, 9]. In [10, 11] the authors utilize Hadamard masks to reduce the acquisition time. In [12] a PMMW imaging system with extended depth-of-field that can produce images with reduced number of samples is presented. CS and Blind Image Deconvolution have been combined in [13]. By end large the resolution of MMW images is small, therefore making their analysis a challenging task. In this paper we propose a novel optimization framework to obtain HR PMMW images from multiple LR observations captured using a simulated CS imaging system based on the ADMM to link the CS and SR problems.

The rest of this paper is organized as follows. The modeling problem is stated in Section 2, and the estimation process in section 3. We demonstrate the effectiveness of the proposed method with experimental results in Section 4 and conclusions are drawn in Section 5.

2. SYSTEM MODELING

In this paper we assume that we have access to a set of Q CS LR observations of the form

$$\mathbf{y}_q = \mathbf{\Phi}\mathbf{z}_q + \mathbf{r}_q \quad q = 1, \ldots, Q, \tag{1}$$

where $\mathbf{y}_q$ is an $M \times 1$ vector representing compressed observations from the LR image $\mathbf{z}_q$, $\mathbf{\Phi}$ is a CS $M \times D$ measurement matrix, $\mathbf{z}_q$ is a column vector of size $D \times 1$ representing the $q-$th LR image and $\mathbf{r}_q$ represents the observation noise. If we define R to be the compression ratio of the measurement system, then R$= M/D$. The sensing matrix $\mathbf{\Phi}$ consists of real entries, or it can be binary. The matrix used in our work is of the binary format, as this can be synthesized physically [9, 10, 11]. In both cases the rows/columns of $\mathbf{\Phi}$ are normalized to 1. We also assume that the LR observations $\mathbf{z}_q$ are related to an HR image $\mathbf{x}$ we seek to estimate by

$$\mathbf{z}_q = \mathbf{A}\mathbf{H}_q\mathbf{C}(\mathbf{s}_q)\mathbf{x} + \mathbf{w}_q = \mathbf{B}_q(\mathbf{s}_q)\mathbf{x} + \mathbf{w}_q, \tag{2}$$

where $\mathbf{x}$ is a column vector of size N we want to recover, $\mathbf{A}$ is a $D \times N$ down-sampling matrix, $D \leq N$. If we define P

978-0-9928626-3-3/15/$31.00 ©2015 IEEE

as the zooming factor, in each dimension of the image, then $N = P^2 D$. $\mathbf{H}_q$ is an $N \times N$ blurring matrix, $\mathbf{C}(\mathbf{s}_q)$ is the $N \times N$ warping matrix corresponding to the motion vector $\mathbf{s}_q = [\theta_q, d_{hq}, d_{vq}]^t$, where θ_q is the rotation angle, d_{hq} and d_{vq} are respectively the horizontal and vertical translations of the $q-$th LR image with respect to the reference frame, and $\mathbf{w}_q$ is the noise corresponding to the LR acquisition process. A detailed description of the explicit form of the $\mathbf{C}(\mathbf{s}_q)$ matrices can be found in [14]. We have written $\mathbf{B}_q(\mathbf{s}_q) = \mathbf{A}\mathbf{H}_q\mathbf{C}(\mathbf{s}_q)$ for simplicity. Using (1) and (2) we can write

$$\mathbf{y}_q = \mathbf{\Phi}\mathbf{B}_q(\mathbf{s}_q)\mathbf{x} + \mathbf{n}_q\,, \text{ for } q = 1, \ldots, Q, \tag{3}$$

where $\mathbf{n}_q$ represents the CS and LR acquisition noise and $\mathbf{x}$ is the HR image we want to estimate. Since $\mathbf{z}_q$ are translated and rotated LR versions of the original image $\mathbf{x}$ (which are assumed to be compressible in a transformed domain) we could estimate the original HR image by first recovering the LR images using CS techniques and then recover the HR image using standard SR techniques on the recovered LR images. To be precise, if we assume that the LR images are sparse in a transformed domain with $\mathbf{z}_q$=$\mathbf{W}\mathbf{a}_q$, we could recover them from the model in (1) by solving

$$\hat{\mathbf{a}}_q = \arg\min_{\mathbf{a}_q} \frac{\eta}{2} \parallel \mathbf{\Phi}\mathbf{W}\mathbf{a}_q - \mathbf{y}_q \parallel^2 + \tau \parallel \mathbf{a}_q \parallel_1, \tag{4}$$

where η, τ are regularization parameters, $\|\,.\,\|$ is the Euclidean norm, and $\|\,.\,\|_1$ the $\ell 1$ norm. Then defining $\hat{\mathbf{z}}_q = \mathbf{W}\hat{\mathbf{a}}_q$ and $\mathbf{s} = (\mathbf{s}_1, \ldots, \mathbf{s}_q)$ we could solve

$$\hat{\mathbf{x}}, \hat{\mathbf{s}} = \arg\min_{\mathbf{x},\mathbf{s}} \left\{ \frac{\beta}{2} \sum_q \parallel \mathbf{B}_q(\mathbf{s}_q)\mathbf{x} - \hat{\mathbf{z}}_q \parallel^2 + \alpha\, Q(\mathbf{x}) + \sum_q (\mathbf{s}_q - \bar{\mathbf{s}}_q)^t \mathbf{\Xi}_q (\mathbf{s}_q - \bar{\mathbf{s}}_q) \right\}, \tag{5}$$

where α and β are non-negative parameters, and the remaining terms are described in details now. $Q(\mathbf{x})$ is the following log regularization term

$$Q(\mathbf{x}) = \sum_{d \in \Delta} \sum_{i=1}^{N} \log(|\omega_d^{\mathbf{x}}(i)|)\,, \tag{6}$$

where $\omega_d^{\mathbf{x}}(i)$ is the i-th pixel of the filtered image $\boldsymbol{\omega}_d^{\mathbf{x}} = \mathbf{F}_d\mathbf{x}$.

$\mathbf{F}_d$ is a high-pass filter operator, and the index $d \in \Delta$ identifies one of the members of the used filter set. In this paper we have used a filter set with elements $\Delta = \{h, v, hv, vh, hh, vv\}$, where h, v represent the first order horizontal and vertical difference filters, hv and vh represent first order differences along diagonals, and hh and vv the horizontal and vertical second order differences. This regularization term favors sparsity of the high-pass filtered images $\mathbf{F}_d\mathbf{x}$, and corresponds to a Super-Gaussian log prior used in blind deconvolution [15]. Finally $\mathbf{\Xi}_q$ is a 3×3 known matrix of regularization parameters and $\bar{\mathbf{s}}_q$ represents the known initial values of registration parameter $\mathbf{s}_q$.

As we will show in the experimental section, combining the sequential optimization problems above into a simultaneous one leads to improved performance, as this enables the better exploitation of the compressibility of the LR observations using the additional information derived from the estimated HR image. Let $\mathbf{a} = (\mathbf{a}_1, \ldots, \mathbf{a}_q)$ and define

$$L(\mathbf{x}, \mathbf{a}, \mathbf{s}) = \frac{\eta}{2} \parallel \mathbf{\Phi}\mathbf{W}\mathbf{a}_q - \mathbf{y}_q \parallel^2 + \tau \parallel \mathbf{a}_q \parallel_1 + \beta \sum_q \parallel \mathbf{B}_q(\mathbf{s}_q)\mathbf{x} - \mathbf{W}\mathbf{a}_q \parallel^2 + \alpha\, Q(\mathbf{x}) + \sum_q (\mathbf{s}_q - \bar{\mathbf{s}}_q)^t \mathbf{\Xi}_q (\mathbf{s}_q - \bar{\mathbf{s}}_q). \tag{7}$$

Then we could approach the compressed-sensing super resolution (CSSR) problem by minimizing $L(\mathbf{x}, \mathbf{a}, \mathbf{s})$ where β is made iteratively large. Alternatively, the approach we follow in this paper, is to solve

$$\min L(\mathbf{x}, \mathbf{a}, \mathbf{s}) \quad \text{s.t.} \quad \mathbf{B}_q(\mathbf{s}_q)\mathbf{x} = \mathbf{W}\mathbf{a}_q\,, \text{for } \; q = 1, \ldots, Q\,, \tag{8}$$

as described in the next section.

3. A SUPER-RESOLUTION FROM COMPRESSED SENSING APPROACH

The constrained optimization problem in (8) is converted into an unconstrained optimization one, and modified to apply ADMM [16, 17]. We define the following augmented Lagrangian functional

$$L(\mathbf{x}, \mathbf{a}, \mathbf{s}, \boldsymbol{\lambda}) = L(\mathbf{x}, \mathbf{a}, \mathbf{s}) + \sum_q \boldsymbol{\lambda}_q^t (\mathbf{B}_q(\mathbf{s}_q)\mathbf{x} - \mathbf{W}\mathbf{a}_q), \tag{9}$$

where $L(\mathbf{x}, \mathbf{a}, \mathbf{s})$ has been defined in (7) and for $q = 1, \ldots, Q$, $\boldsymbol{\lambda}_q$ are $D \times 1$ Lagrangian multiplier vectors with $\boldsymbol{\lambda} = (\boldsymbol{\lambda}_1, \ldots, \boldsymbol{\lambda}_Q)$. The ADMM gives rise to the following iterative sequence of unconstrained problems,

$$\mathbf{x}^{k+1} = \arg\min_{\mathbf{x}} L(\mathbf{x}, \mathbf{a}^k, \mathbf{s}^k, \boldsymbol{\lambda}^k)\,, \tag{10}$$

$$\mathbf{a}^{k+1} = \arg\min_{\mathbf{a}} L(\mathbf{x}^{k+1}, \mathbf{a}, \mathbf{s}^k, \boldsymbol{\lambda}^k) \tag{11}$$

$$\mathbf{s}^{k+1} = \arg\min_{\mathbf{s}} L(\mathbf{x}^{k+1}, \mathbf{a}^{k+1}, \mathbf{s}, \boldsymbol{\lambda}^k) \tag{12}$$

$$\boldsymbol{\lambda}_q^{k+1} = \boldsymbol{\lambda}_q^k - \beta[\mathbf{B}_q(\mathbf{s}_q^{k+1})\mathbf{x}^{k+1} - \mathbf{W}\mathbf{a}_q^{k+1}] \quad q = 1, \ldots, Q, \tag{13}$$

where k is the iteration number. Let us now describe the estimation process. The calculation of each $\boldsymbol{\lambda}_q^{k+1}$ is straightforward. The function $\rho(s) = \log|s|$ in (6) is symmetric around 0, and $\rho(\sqrt{s})$ is concave and increasing for $s \in [0, \infty)$ [15]. So, it can be represented as (see [18])

$$\rho(s) = \inf_{\xi > 0} \frac{1}{2}\xi s^2 - \rho^*(\frac{1}{2}\xi)\,, \tag{14}$$

where $\rho^*(\frac{1}{2}\xi)$ is the concave conjugate function

$$\rho^*(\frac{1}{2}\xi) = \inf_{s > 0} \frac{1}{2}\xi s^2 - \rho(s)\,. \tag{15}$$

It is shown in [15] that the infimum in (14) is achieved when $\xi = \rho'(s)/s$. Consequently, for the regularization term $Q(\mathbf{x})$ in (7), we can write

$$Q(\mathbf{x}) \leq R(\mathbf{x}, \boldsymbol{\xi}) = \frac{1}{2} \sum_{d \in \Delta} \mathbf{x}^t \mathbf{F}_d^t \boldsymbol{\Omega}_d \mathbf{F}_d \mathbf{x} - \sum_{d \in \Delta} \sum_{i=1}^{N} \rho^*(\frac{1}{2} \xi_d(i)) \tag{16}$$

where $\boldsymbol{\xi} = (\boldsymbol{\xi}_1, \ldots, \boldsymbol{\xi}_Q)$, $\boldsymbol{\xi}_q = (\xi_q(1), \ldots, \xi_q(N))$ for $q = 1, \ldots, Q$, with all its components positive, and $\boldsymbol{\Omega}_d$ is a diagonal matrix with entries

$$\Omega_d(i,i) = \xi_d(i). \tag{17}$$

For a given $\mathbf{x}$, the first inequality in (16) becomes an equality if (see [15] for details),

$$\xi_d^{\mathbf{x}}(i) = \frac{1}{|\omega_d^{\mathbf{x}}(i)|^2 + \epsilon}\,, \tag{18}$$

where $\omega_d^{\mathbf{x}}(i)$ is defined from $\mathbf{x}$ as above, $\epsilon > 0$ is added to avoid division by zero. Then we can apply standard Majorization-Minimization (MM) methods [19]. Given $\mathbf{x}^k, \mathbf{a}^k, \mathbf{s}^k$ and defining

$$L^k(\mathbf{x}) = \frac{\beta}{2} \sum_q \parallel \mathbf{B}_q(\mathbf{s}_q^k)\mathbf{x} - \mathbf{W}\mathbf{a}_q^k \parallel^2 + \sum_q \boldsymbol{\lambda}_q^{k\,t}(\mathbf{B}_q(\mathbf{s}_q^k)\mathbf{x} - \mathbf{W}\mathbf{a}_q^k) \tag{19}$$

it can be easily shown that

$$L^k(\mathbf{x}^k) + \alpha Q(\mathbf{x}^k) \geq L^k(\mathbf{x}^{k+1}) + \alpha Q(\mathbf{x}^{k+1}) \tag{20}$$

where

$$\mathbf{x}^{k+1} = \arg\min_{\mathbf{x}} \left\{ \frac{\beta}{2} \sum_q \parallel \mathbf{B}_q(\mathbf{s}_q^k)\mathbf{x} - \mathbf{W}\mathbf{a}_q \parallel^2 + \alpha R(\mathbf{x}, \boldsymbol{\xi}^{\mathbf{x}^k}) + \sum_q \boldsymbol{\lambda}_q^{k\,t}(\mathbf{B}_q(\mathbf{s}_q^k)\mathbf{x} - \mathbf{W}\mathbf{a}_q^k) \right\} \tag{21}$$

Then, the optimization step in (10) produces the following linear equation for $\mathbf{x}^{k+1}$

$$\left[\beta \sum_q \mathbf{B}^{k\,t}_q(\mathbf{s}_q^k)\mathbf{B}_q^k(\mathbf{s}_q^k) + \alpha \sum_{d \in \Delta} \mathbf{F}_d^t \boldsymbol{\Omega}_d^k \mathbf{F}_d \right] \mathbf{x}^{k+1} = \sum_q \mathbf{B}_q^k(\mathbf{s}_q^k)^t \left[\beta \mathbf{W}\mathbf{a}_q^k - \lambda_q^k \right] \tag{22}$$

where, ($\epsilon > 0$ is included to avoid division by zero)

$$\Omega_d^k(i,i) = \frac{1}{\epsilon + |\omega_d^{\mathbf{x}^k}(i)|^2} \tag{23}$$

The optimization step in (11) for each $\mathbf{a}_q$ produces

$$\mathbf{a}_q^{k+1} = \arg\min_{\mathbf{a}_q} \left\{ \frac{\eta}{2} \parallel \boldsymbol{\Phi}\mathbf{W}\mathbf{a}_q - \mathbf{y}_q \parallel^2 + \tau \parallel \mathbf{a}_q \parallel_1 + \frac{\beta}{2} \parallel \mathbf{B}_q^k(\mathbf{s}_q^k)\mathbf{x}^{k+1} - \mathbf{W}\mathbf{a}_q \parallel^2 - \boldsymbol{\lambda}_q^{k\,t}(\mathbf{B}_q^k(\mathbf{s}_q^k)\mathbf{x} - \mathbf{W}\mathbf{a}_q) \right\} \tag{24}$$

Algorithm 1 Compressive Sensing Super Resolution (CSSR)

Require: Values α, β, τ, η, $\boldsymbol{\Xi}_q$ and $\mathbf{s}_q^0$, for $q = 1, \ldots, Q$.
Initialize $\mathbf{a}^0$, $\mathbf{s}^0$, $\boldsymbol{\lambda}^0$, $\boldsymbol{\Omega}^0 = \{\boldsymbol{\Omega}_d^0, d \in \Delta\}$,
$k = 0$
while convergence criterion is not met **do**
1. Calculate $\mathbf{x}^{k+1}$ by solving (22)
2. For $d \in \Delta$, calculate $\boldsymbol{\Omega}_d^{k+1}$ using (23)
3. For $q = 1, \ldots, Q$, calculate $\mathbf{a}_q^{k+1}$ using (26)
4. For $q = 1, \ldots, Q$, calculate $\mathbf{s}_q^{k+1}$ using (28)
5. For $q = 1, \ldots, Q$, update $\boldsymbol{\lambda}_q^{k+1}$ using (13)
6. Set $k = k + 1$
end while
return $\mathbf{x}$

which is equivalent to

$$\mathbf{a}_q^{k+1} = \arg\min_{\mathbf{a}_q} \left\{ \frac{\eta}{2} \parallel \boldsymbol{\Phi}\mathbf{W}\mathbf{a}_q - \mathbf{y}_q \parallel^2 + \frac{\beta}{2} \parallel \mathbf{B}_q^k(\mathbf{s}_q^k)\mathbf{x}^{k+1} - \boldsymbol{\lambda}_q^k - \mathbf{W}\mathbf{a}_q \parallel^2 + \tau \parallel \mathbf{a}_q \parallel_1 \right\} \tag{25}$$

The above equation can be rewritten as

$$\mathbf{a}_q^{k+1} = \arg\min_{\mathbf{a}_q} \parallel \boldsymbol{\Phi}'\mathbf{W}\mathbf{a}_q - \mathbf{J}' \parallel^2 + \tau \parallel \mathbf{a}_q \parallel_1 \tag{26}$$

where

$$\mathbf{J}' = \begin{bmatrix} \sqrt{\frac{\eta}{2}}\mathbf{y}_q \\ \sqrt{\frac{\beta}{2}}(\mathbf{B}_q^k(\mathbf{s}_q^k)\mathbf{x}^{k+1} - \boldsymbol{\lambda}_q^k) \end{bmatrix} \text{ and } \boldsymbol{\Phi}' = \begin{bmatrix} \sqrt{\frac{\eta}{2}}\boldsymbol{\Phi} \\ \sqrt{\frac{\beta}{2}}\mathbf{I} \end{bmatrix} \tag{27}$$

with $\mathbf{I}$ the $D \times D$ identity matrix.

The above optimization problem can be solved using the algorithm in [20].

To update the registration parameters, we need to minimize (12) for $\mathbf{s}_q$; however, we have experimentally observed that a fast and reliable estimation of the registration parameters can be obtained by estimating warping parameters from the upsampled reconstructed LR observations with respect to the estimated HR image. Replacing $\bar{\mathbf{s}}_q$ by $\mathbf{s}_q^k$, the minimization problem becomes

$$\mathbf{s}_q^{k+1} = \arg\min_{\mathbf{s}_q} \left[\frac{\beta}{2} \parallel \mathbf{C}(\mathbf{s}_q)\mathbf{x}^{k+1} - [\mathbf{A}\mathbf{H}_q]^t \mathbf{W}\mathbf{a}_q^{k+1} \parallel^2 + (\mathbf{s}_q - \mathbf{s}_q^k)^t \boldsymbol{\Xi}_q (\mathbf{s}_q - \mathbf{s}_q^k) \right]. \tag{28}$$

We follow a similar approach to the one utilized in [14] to solve the above optimization problem.

The complete CSSR algorithm is presented in Algorithm 1

4. EXPERIMENTAL RESULTS

To evaluate the proposed algorithm, three experiments were carried out. The first two analyze the behavior of the proposed CSSR method on synthetic data for varying parameters, using the cameraman and Lena images shown in Figure 1. They are degraded as follows: they are first warped using random displacement vectors to account for horizontal, verti-

(a) Cameraman

(b) Lena

Fig. 1. Original Images

Table 1. Performance comparison for SR algorithms with proposed CSSR algorithm, with P=4, SNR=40dB, Q=4 and for CSSR R=1.0. In bold are the highest PSNR values.

Img	Alg / Var	BI	VB	SnS	FRSR	RSR	CSSR
		PSNR Values					
Cam	3	20.5	21.8	22.2	21.1	20.5	**24.6**
	5	20.5	21.8	22.1	20.9	20.4	**24.1**
	7	20.5	21.7	21.8	20.7	20.4	**23.7**
Len.	3	21.0	26.0	26.4	21.9	21.7	**27.9**
	5	21.1	26.3	26.9	21.8	21.7	**27.3**
	7	21.1	26.0	**26.7**	23.4	21.7	**26.7**

cal and rotational displacements. They are then blurred with Gaussian blur, with variable variance and down-sampled by a factor P. Finally they are compressed using Φ, with variable ratios (R), and white Gaussian noise is added to the CS observations with SNR=40dB. Q different observations are generated. The performance measure we used is the Peak Signal to Noise Ratio, PSNR. Stopping criteria are met when either $\frac{norm(\mathbf{x}^k - \mathbf{x}^{k-1})}{norm(\mathbf{x}^{k-1})} \leq 10^{-3}$, or the maximum number of iterations, being thirty, is reached. The 3-level Haar wavelet transform is used as the transform basis W, and a circulant Toeplitz matrix Φ with entries drawn from a Bernoulli distribution serves as a measurement matrix.

In the first experiment, we compare our proposed method with the following existing SR methods: Bicubic Interpolation (BI), SR using a variational approach [21] (VB), SR using sparse and non-sparse priors [14] (SnS), a fast and robust SR [22] (FRSR), and a robust SR method [23](RSR). The number of input LR images was Q=4, with resolution increase $P = 4$. We used compression ratio R$= 1.0$ to compare with the above mentioned algorithms which do not use compressed observations. Results are tabulated in Table 1.

In the second experiment, we investigate the performance of our method for variable compression rates, R. For all images we used Gaussian blur of variance 3, zooming factor P=1, and SNR=40dB and Q=3. The results are tabulated in Table 2, for the two images used in our study. Figure 2(a), shows the estimated cameraman image using CSSR, with P=1, R=0.5, Q=3, Blur Var=3.

Table 2. Performance of CSSR algorithm via compression ratio. P=1, Blur Var=3, SNR=40dB, Q=3.

Ratio	0.4	0.5	0.6	0.7	0.8	0.9	1.0
Image	PSNR Values						
Cam	25.1	25.4	25.6	25.7	25.8	25.8	25.9
Lena	28.2	29.0	29.7	30.1	30.4	30.6	30.8

In the third experiment, four real PMMW images of a person were acquired successively, see Figure 2(b). These observations were synthetically compressed using R=0.6, 0.8 and 1.0. For each R, the four observations were utilized to estimate one HR image with $P = 2$. The estimated image using bilinear interpolation from one reconstructed LR image is shown in Figure 2(c), and the estimated using CSSR is shown in Figure 2(d), both using P=2 and R=0.8. Notice that although both SR images have poor quality the one obtained by our method looks smoother and shows additional details. This good performance for PMMWIs is expected to be very useful in threat detection, one of the main usages of these images.

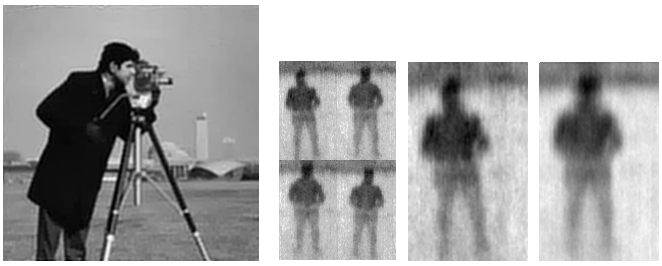

(a) (b) (c) (d)

Fig. 2. (a) Estimated Cameraman image using CSSR, P=1, R=0.5, (b) Four noisy real PMMW observations, (c) Bilinear interpolation from one reconstructed LR image, (d) Estimated image using CSSR, R=0.8, P=2.

5. CONCLUSIONS

In this paper we have proposed a framework to obtain HR images from compressed LR observations which has been applied to simulated CS PMMW images obtained from real PMMW images. An optimization framework based on the combination of existing CS reconstruction algorithms and ADMM has been proposed. The method included the automatic estimation of the registration parameters. Its effectiveness has been demonstrated experimentally on real and synthetic images. In future work we will examine the applicability of the proposed method to improve threat detection rates on PMMW images.

REFERENCES

[1] L. Yujiri, M. Shoucri, and P. Moffa, "Passive millimeter wave imaging," *Microwave Magazine, IEEE*, vol. 4, no. 3, pp. 39–50, Sept 2003.

[2] H. Chen, S. Lee, R. Rao, M. Slamani, and P. Varshney, "Imaging for concealed weapon detection: a tutorial overview of development in imaging sensors and processing," *Signal Processing Magazine, IEEE*, vol. 22, no. 2, pp. 52–61, 2005.

[3] C. Zheng, X. Yao, A. Hu, and J. Miao, "A passive millimeter-wave imager used for concealed weapon detection," *Progress In Electromagnetics Research B*, vol. 46, pp. 379–397, 2013.

[4] J. Yang, J. Wang, and L. Li, "A new algorithm for passive millimeter-wave image enhancement," in *Signal Processing Systems (ICSPS), 2010 2nd International Conference on*. IEEE, 2010, vol. 3, pp. V3–507.

[5] Y. Li, Y. Li, J. Chen, and Y. Hou, "Passive millimeter-wave image restoration based on improved algorithm of nonlinear extrapolation in frequency space," *International Journal of Digital Content Technology and its Applications*, vol. 5, no. 5, pp. 42–49, 2011.

[6] H. Lee, D. Lee, S. Yeom, J. Son, V. Guschin, and S. Kim, "Passive millimeter wave imaging and analysis for concealed object detection," in *Data Mining and Intelligent Information Technology Applications (ICMiA), 2011 3rd International Conference on*. IEEE, 2011, pp. 98–101.

[7] P. Chen, T. Zou, J. Chen, Z. Gao, and J. Xiong, "The application of improved pso algorithm in pmmw image ostu threshold segmentation," in *Applied Mechanics and Materials*. Trans Tech Publ, 2015, vol. 721, pp. 779–782.

[8] W. L. Chan, K. Charan, D. Takhar, K. F. Kelly, R.G. Baraniuk, and D.M. Mittleman, "A single-pixel terahertz imaging system based on compressed sensing," *Applied Physics Letters*, vol. 93, no. 12, pp. 121105–121105–3, Sep 2008.

[9] A. Heidari and D. Saeedkia, "A 2d camera design with a single-pixel detector," in *Infrared, Millimeter, and Terahertz Waves, 2009. IRMMW-THz 2009. 34th International Conference on*, Sept 2009, pp. 1–2.

[10] N. Gopalsami, S. Liao, T. W Elmer, E. R Koehl, A. Heifetz, A. C Raptis, L. Spinoulas, and A. K Katsaggelos, "Passive millimeter-wave imaging with compressive sensing," *OPTICAL ENGINEERING*, vol. 51, no. 9, SEP 2012.

[11] N. Gopalsami, TW. Elmer, S. Liao, R. Ahern, A. Heifetz, A. Raptis, M. Luessi, D. Babacan, and AK. Katsaggelos, "Compressive sampling in passive millimeter-wave imaging," in *SPIE Defense, Security, and Sensing*. International Society for Optics and Photonics, 2011, pp. 80220I–80220I.

[12] V. Patel and J. Mait, "Passive millimeter-wave imaging with extended depth of field and sparse data," in *Acoustics, Speech and Signal Processing (ICASSP), 2012 IEEE International Conference on*. IEEE, 2012, pp. 2521–2524.

[13] B. Amizic, L. Spinoulas, R. Molina, and A.K. Katsaggelos, "Compressive blind image deconvolution," *Image Processing, IEEE Transactions on*, vol. 22, no. 10, pp. 3994–4006, Oct 2013.

[14] S. Villena, M. Vega, S.D. Babacan, R. Molina, and A.K. Katsaggelos, "Bayesian combination of sparse and non-sparse priors in image super resolution," *Digital Signal Processing*, vol. 23, no. 2, pp. 530–541, 2013.

[15] S. Babacan, R. Molina, M. Do, and A. K. Katsaggelos, "Bayesian blind deconvolution with general sparse image priors," in *Computer Vision–ECCV 2012*, pp. 341–355. Springer, 2012.

[16] S. Boyd, N. Parikh, E. Chu, B. Peleato, and J. Eckstein, "Distributed optimization and statistical learning via the alternating direction method of multipliers," *Foundations and Trends® in Machine Learning*, vol. 3, no. 1, pp. 1–122, 2011.

[17] Y.-H. Xiao and Z.-F. Jin, "An alternating direction method for linear-constrained matrix nuclear norm minimization," *Numerical Linear Algebra with Applications*, vol. 19, no. 3, pp. 541–554, 2012.

[18] R Tyrrell Rockafellar, *Convex analysis*, Number 28. Princeton university press, 1997.

[19] K. Lange, *Optimization*, Springer-Verlag, 2013.

[20] K. Koh, S. J Kim, and S. P Boyd, "An interior-point method for large-scale l1-regularized logistic regression.," *Journal of Machine learning research*, vol. 8, no. 8, pp. 1519–1555, 2007.

[21] S.D. Babacan, R. Molina, and A.K. Katsaggelos, "Variational bayesian super resolution," *IEEE Transactions on Image Processing*, vol. 20, no. 4, pp. 984–999, 2011.

[22] S. Farsiu, M.D. Robinson, M. Elad, and P. Milanfar, "Fast and robust multiframe super resolution," *IEEE Transactions on Image Processing*, vol. 13, no. 10, pp. 1327–1344, 2004.

[23] A. Zomet, A. Rav-Acha, and S. Peleg, "Robust super-resolution," in *Computer Vision and Pattern Recognition, 2001. CVPR 2001. Proceedings of IEEE Computer Society Conference on*, 2001, vol. 1, pp. I–645–I–650.